Local Dynamics of DNA Probed with Optical Absorption Spectroscopy of Bound Ethidium Bromide

Antonio Cupane, Caterina Bologna, Ottavio Rizzo, Eugenio Vitrano, and Lorenzo Cordone
Istituto Nazionale di Fisica della Materia and Istituto di Fisica dell'Università di Palermo, I-90123 Palermo, Italy

ABSTRACT We have studied the local dynamics of calf thymus double-helical DNA by means of an "optical labeling" technique. The study has been performed by measuring the visible absorption band of the cationic dye ethidium bromide, both free in solution and bound to DNA, in the temperature interval 360–30 K and in two different solvent conditions. The temperature dependence of the absorption line shape has been analyzed within the framework of the vibronic coupling theory, to extract information on the dynamic properties of the system; comparison of the thermal behavior of the absorption band of free and DNA-bound ethidium bromide gave information on the local dynamics of the double helix in the proximity of the chromophore. For the dye free in solution, large spectral heterogeneity and coupling to a "bath" of low-frequency (soft) modes is observed; moreover, anharmonic motions become evident at suitably high temperatures. The average frequency of the soft modes and the amplitude of anharmonic motions depend upon solvent composition. For the DNA-bound dye, at low temperatures, heterogeneity is decreased, the average frequency of the soft modes is increased, and anharmonic motions are hindered. However, a new dynamic regime characterized by a large increase in anharmonic motions is observed at temperatures higher than ~280 K. The DNA double helix therefore appears to provide, at low temperatures, a rather rigid environment for the bound chromophore, in which conformational heterogeneity is reduced and low-frequency motions (both harmonic vibrations and anharmonic contributions) are hindered. The system becomes anharmonic at ~180 K; however, above ~280 K, anharmonicity starts to increase much more rapidly than for the dye free in solution; this can be attributed to the onset of wobbling of the dye in its intercalation site, which is likely connected with the onset of (functionally relevant) DNA motions, involving local opening/unwinding of the double helix. As shown by parallel measurements of the melting curves, these motions precede the melting of the double helix and depend upon solvent composition much more than does the melting itself.

INTRODUCTION

The temperature dependence of the optical absorption lineshape of a chromophore embedded in a matrix gives information on the local dynamics of the system. In particular, coupling of the electronic transition that gives rise to the observed absorption band with high-frequency vibrational modes and with a "bath" of soft modes, as well as the onset, at suitably high temperatures, of nonharmonic motions have recently been shown for heme proteins and other metalloproteins, by the use of this technique (Di Pace et al., 1992; Cupane et al., 1993, 1994, 1995a,b; Boffi et al., 1994; Leone et al., 1994, 1996; Militello et al., 1995; Melchers et al., 1996). These works open the possibility of using an "optical labeling" technique to study the local dynamic properties of biological macromolecules that do not contain per se a chromophore exhibiting a suitable absorption band. The idea is to selectively bind an optical probe to the macromolecule, thus forming a stable complex, and to study the thermal evolution of the absorption spectrum of the probe. Comparison of the dynamics of the chromophore free in solution and bound to the macromolecule will give information on the local dynamics, in the proximity of the chromophore, of the macromolecule itself.

On the other hand, studies on the local dynamics of nucleic acids in solution and of drug-nucleic acid complexes are of considerable interest, because local structural fluctuations of the polymer may play a role in the replication and transcription of DNA and in the antitumor activity of several drugs.

The cationic dye ethidium bromide (2,7-diamino-10-ethyl-9-phenyl-phenanthridinium bromide, EB) is known to intercalate between base pairs in double-helical DNA, thus forming very stable complexes. The binding geometry is known at atomic resolution (Tsai et al., 1977; Jain et al., 1977), and the binding constants in various solvents have been measured (Baldini and Varani, 1985; Varani et al., 1987); molecular mechanics and harmonic dynamics calculations of the DNA/EB complex are also available (Lybrand and Kollman, 1985; Rudolph and Case, 1989). Moreover, the absorption spectrum of EB exhibits a rather intense visible band ($\epsilon \approx 5900\ M^{-1}\ cm^{-1}$ at 480 nm in water at room temperature), well separated from other bands of the chromophore or of the host macromolecule. The DNA-EB system therefore seems very promising for applying the "optical labeling" technique described above for studies of the local dynamic properties of double-helical DNA. It should also be mentioned that EB has frequently been used as a fluorescent probe to investigate the dynamic properties of DNA (see, e.g., Härd et al., 1989; Nuutero et al., 1994;

Received for publication 6 February 1997 and in final form 30 April 1997.
Address reprint requests to Dr. Antonio Cupane, Istituto di Fisica dell'Università di Palermo, via Archirafi 36, 90123 Palermo, Italy. Tel.: +39-91-6171708; Fax: +39-91-6162461; E-mail: cupane@ist.fisica.unipa.it.

0006-3495/97/08/959/07 $2.00

Collini et al., 1995). In particular, time-resolved measurements of the fluorescence anisotropy decay in the picosecond time scale have been used to probe the "wobble" of the drug in its intecalation site (Magde et al., 1983; Shibata et al., 1985; Härd et al., 1989); these data are of particular relevance to the present study, because our technique is able to monitor only nuclear motions that take place with respect to the planar structure of the chromophore (Melchers et al., 1996) rather than overall motions of the chromophore-macromolecule complex (e.g., torsional dynamics of the double helix).

In this work we have measured the visible band of EB both free in solution and bound to calf thymus DNA in the temperature range 360–30 K and in two different solvents. The temperature dependence of the absorption lineshape has been successfully analyzed within the framework of the vibronic coupling theory (see, e.g., Cupane et al., 1995b) and gives information on the local dynamic properties of the system. Comparison of the chromophore dynamics in the free and DNA-bound states, in turn, gives information on the local dynamic properties of the double helix. The DNA double helix appears to provide, at low temperatures, a rather rigid environment for the bound chromophore, in which conformational heterogeneity is reduced and low-frequency motions (both harmonic vibrations and anharmonic motions) are hindered. A large anharmonicity increase is observed at ~280 K and can be attributed to increased "wobbling" of the drug in its intercalation site, in connection with the onset of local opening/unwinding of the double helix. As shown by parallel measurements of the melting curves, these motions precede the melting of the double helix and depend upon solvent composition much more than does the melting itself.

MATERIALS AND METHODS

Samples

DNA sodium salt, highly polymerized, from calf thymus was purchased from Sigma Chemical Co. (St. Louis, MO) and was used without further purification.

EB was purchased from Sigma-Aldrich (Milan, Italy); ethylene glycol (puriss.) and glycerol (anhydrous) were purchased from Fluka Chimica (Milan, Italy).

Optical spectra of EB free in solution were measured on samples containing 10^{-2} M K-phosphate buffer (pH 7, in water at room temperature), 1.8×10^{-4} M ethidium bromide, and 80% ethylene glycol/water or 90% glycerol/water. The monomer $\rightleftarrows$ dimer aggregation constant for EB in water at room temperature has been reported to be ~100 M^{-1} (Bresloff and Crothers, 1975), so that at the concentration used, more than 96.5% of the dye is expected to be in monomeric form. The aggregation state in the actual solvents used was directly checked by measuring the optical spectra of EB at various concentrations in the range 1.25×10^{-5}-2.5×10^{-4} M. Results showed that spectra taken at various concentrations were different only for a scale factor, therefore excluding the presence of a detectable fraction of EB dimers in our experimental conditions.

Optical spectra of EB bound to DNA were measured on samples containing 10^{-2} M K-phosphate buffer (pH 7, in water at room temperature), 5×10^{-5} M ethidium bromide, 9.6×10^{-4} M DNA (in [P]), and 80% ethylene glycol/water or 90% glycerol/water. The above solutions were left overnight under gentle stirring at 4°C; before the measurements were begun, the solutions were brought to room temperature and filtered through a 1.2-μ Millipore filter. At the concentrations used, the ratio [DNA]/[EB] is ~19, i.e. one dye molecule for every ~10 base pairs. The rather high value of the equilibrium constant for the association of ethidium bromide to DNA ($K_{eq} \simeq 10^5$ M^{-1}) and the rather low value of the dimerization constant ($K_D \simeq 100$ M^{-1}) ensure that under our experimental conditions, the fraction of unbound dye is negligible.

Optical spectroscopy

Absorption spectra (650–350 nm) were measured with a JASCO Uvidec 650 spectrophotometer, set to 0.7-nm bandwidth, 0.4-s integration time, and 100 nm/min scan speed, corresponding to a spectral resolution of ~30 cm^{-1} (at 500 nm); data were recorded at 0.4-nm intervals.

The experimental setup for optical absorption measurements at cryogenic temperatures has already been reported (Cordone et al., 1986). Samples, in 1-cm optical path metacrylate cuvettes, were "quickly" (cooling rate $\geq$ 5 K/min) brought to 150 K and left to equilibrate; measurements at various temperatures were then performed by cooling or heating at a rate of 1.5 K/min and allowing 10 min of equilibration at each temperature; thermal cycling excluded the presence of hysteresis effects. This procedure was necessary to avoid the development of large scattering intensity in the DNA-containing samples when approaching T = 180 K from higher temperatures. This effect (the study of which is, however, beyond the purpose of the present work) is likely due to the slow formation of high-molecular-weight aggregates at temperatures near the glass transition temperature of the solvent, and is prevented if the transition region is crossed quickly enough because, at lower temperatures, the solvent becomes a glass with almost infinite viscosity. The procedure described above enabled us to have homogeneous and transparent samples throughout the whole temperature range investigated. The baseline measured at room temperature was subtracted from each spectrum; indeed, in the spectral region of interest, the baseline does not depend upon temperature.

Melting curves

DNA melting curves were measured from the absorption at 260 nm. Samples were identical to those used for the low temperature absorption experiments; for this reason, 1-mm pathlength quartz cuvettes were used. A linear correction was applied to absorbance values, to account for the thermal expansion of the sample.

Spectral analysis

Fig. 1 shows the spectra of EB free in solution (80% ethylene glycol/water, *left panel*) and bound to DNA (80% ethylene glycol/water, *right panel*), at room temperature and at T = 30 K. The spectra consist of a single broad band centered at ~500 nm. This band is attributed to a single $\pi \rightarrow \pi^*$ electronic transition within the phenanthridinium ring (transition 1–2, in the terminology of Giacomoni and LeBret, 1973); the very weak transitions 1–3 and 1–4 are blue-shifted by 3,500 and 10,700 cm^{-1}, respectively, and therefore are not likely to contribute to the width of the band. We attribute the observed bandwidth to the combined effects of spectral heterogeneity and vibrational coupling; the vibronic structure of the band clearly appears in the low temperature spectrum of the DNA-bound dye (see Fig. 1, *right panel*). It should also be noted that the red edge of the bands is almost perfectly Gaussian; although EB does not radiate as an isolated molecule, but experiences collisions and other interactions, the excited-state lifetime remains such that the homogeneous, Lorentzian broadening does not contribute significantly to the observed bandwidth.

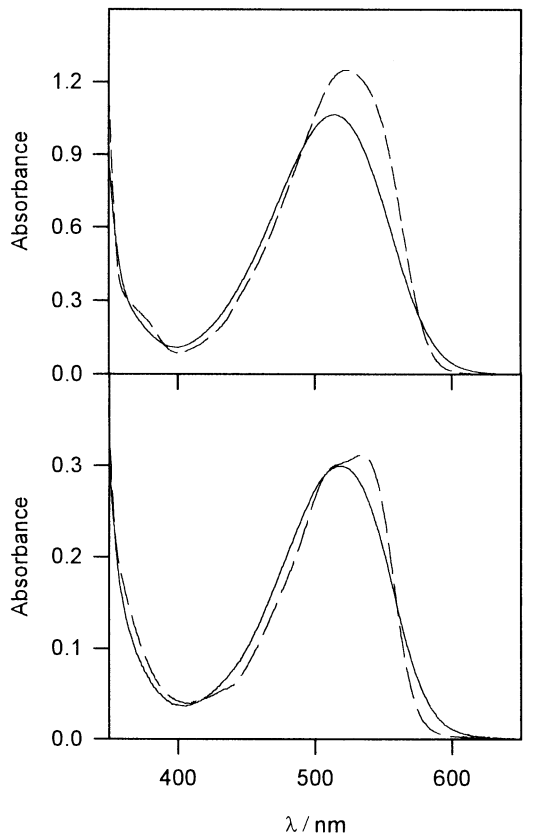

FIGURE 1 Visible absorption spectra of EB free in solution (*top*) and bound to DNA (*bottom*). ——, T = 300 K; – – –, T = 30 K. For both panels the solvent is 80% ethylene glycol/water.

We therefore fit the experimental spectra with the following expression (Cupane et al., 1995b):

$$A(\nu) = M\nu \sum_{\{m_i\}} \left[\prod_i^{N_h} \frac{S_i^{m_i} e^{-S_i}}{m_i!} \right] \times \frac{1}{\sigma(T)} \times \exp\left\{ \frac{[\nu - \nu_0(T) - \sum_i^{N_h} m_i \nu_i]^2}{2\sigma^2(T)} \right\} \quad (1)$$

where M is a constant proportional to the square of the electric dipole moment; the product extends to all high-frequency vibrational modes (i.e., with $h\nu_j > k_B T$) coupled to the electronic transition and the sum to all possible combinations of m_j phonon events in the various high-frequency vibrational modes j; ν_j and S_j are the frequency and linear coupling constant of the jth high-frequency mode, and $\nu_0(T)$ is the peak frequency of the transition. According to Eq. 1, the observed spectrum results from the superposition of a series of Gaussians that includes all possible combinations of multiphonon excitations of the various high-frequency modes; the displacement of the individual Gaussians from the zero phonon line position reflects the energy lost to the vibrational modes. The coupling of the electronic transition with high-frequency modes is responsible for the vibronic structure of the band; in the present case of a $\pi \rightarrow \pi^*$ electronic transition, the high-frequency modes are essentially in plane vibrations of the chromophore macrocycle.

Both spectral heterogeneity and coupling of the electronic transition to a "bath" of low frequency modes of the matrix surrounding the chromophore contribute to the Gaussian halfwidth σ. If one treats the low-frequency bath within the Einstein harmonic oscillator approximation, the temperature dependence of σ can be expressed as

$$\sigma^2 = NS\langle\nu\rangle^2 \coth(h\langle\nu\rangle/2k_BT) + \sigma_{in}^2 \quad (2)$$

In Eq. 2, $\langle\nu\rangle$ and S are the average frequency and linear coupling constant of the low-frequency bath, N is the number of soft modes, and k_B is Boltzmann's constant; the (temperature-independent) term σ^2_{in} takes into account spectral heterogeneity. In the presence of quadratic coupling parameter ν_0 also becomes temperature dependent; within the harmonic approximation, its thermal behavior can be expressed as

$$\nu_0 = \nu_{00} - 1/4\, N\langle\nu\rangle(1 - R)\coth(h\langle\nu\rangle/2k_BT) + C \quad (3)$$

where R is the effective quadratic coupling constant, ν_{00} is the frequency of the purely electronic (0–0) transition, and C takes into account other temperature-independent contributions to the peak position of the band. The temperature dependence of the peak frequency and of the Gaussian width therefore gives information on the local dynamics in the proximity of the chromophore; low-frequency vibrations of the macrocycle, as well as motions of the matrix surrounding the chromophore, are likely to contribute to the low-frequency bath coupled to the electronic transition.

In the analysis of the experimental spectra, M, ν_0, σ, and S_j were fitting parameters. The coupling with only three high-frequency modes was considered, namely: ν_1 = 550 cm^{-1}, ν_2 = 1340 cm^{-1}, ν_3 = 2000 cm^{-1}. We recall that a limit to our resolution of vibronic structure is imposed by the intrinsic width of the Gaussian line, which remains around 400 cm^{-1}, even at low temperature. Therefore, ν_1 = 550 cm^{-1} must be taken as an average mode accounting for the coupling of the electronic transition with "high-frequency" vibrational modes of frequency less than 1000 cm^{-1}. ν_2 = 1340 cm^{-1} is clearly seen in the UV resonance Raman spectra of free and DNA-bound EB (Chinski et al., 1976), as well as in the low-temperature fluorescence spectra (Baldini and Vegetti, 1989) and in the second-derivative absorption spectra at low temperatures (present work, not shown); however, in view of the above argument, contributions from nearby modes at 1600 and 1050 cm^{-1} (Chinski et al., 1976) are also included in this "mode." The coupling with ν_3 = 2000 cm^{-1} is also detected as a small shoulder in the low-temperature absorption spectra (see Fig. 1) and consequently as a minimum in the second-derivative spectra; it may be taken as representative of the coupling with all vibrational modes at frequencies greater than ~1600 cm^{-1}. In agreement with the findings of Chinski et al. (1976), equal ν_j values have been used for the free and DNA-bound dye.

A further Gaussian, centered at ~26,000 cm^{-1}, was added to the fits to take into account contributions from the nearby 1–3 and 1–4 transitions.

A fitting of the 30 K spectrum of EB bound to DNA in 80% ethylene glycol/water in terms of Eq. 1 is shown in Fig. 2, and the residuals are reported in the upper panel; the fitting quality is excellent, and is improved by increasing the temperature. Fittings of comparable quality are obtained for the free and DNA-bound chromophore in both solvents used. Values of the parameters that characterize the coupling of the electronic transition with high-frequency modes are reported in Table 1. Data in Table 1 deserve some comments:

1. Values of the coupling constants to the "modes" at 550 and 1340 cm^{-1} are on the order of 1 and 0.7, respectively. Such large values should not be considered unlikely, in view of the average nature of these "modes" (see discussion above).

2. The coupling constant of the "mode" at 2000 cm^{-1} is in the range 0.05–0.1. This value is typical for the coupling of $\pi \rightarrow \pi^*$ transitions with in-plane vibrational modes of organic macrocycles (Schomacker and Champion, 1986).

3. In agreement with expectations of the literature (Schomacker and Champion, 1989; Cupane et al., 1996), no relevant temperature dependence of coupling constants is observed; in fact, eventual variations of S values are within ±5%. For this reason, S values were taken to be constant in the fittings of the spectra at various temperatures.

4. No relevant differences were observed between S values relative to bound or free chromophore in the two solvents (although a small increase,

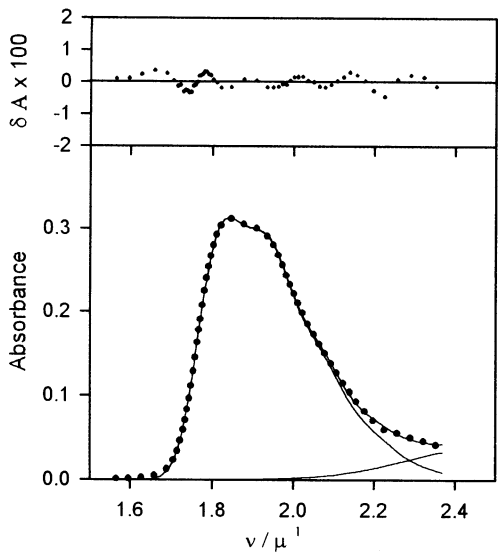

FIGURE 2 Deconvolution of the 30 K spectrum of DNA-bound EB in terms of Eq. 1. The dots are the experimental points (for the sake of clarity, not all of the measured points have been reported); the continuous lines are the theoretical profiles. The residuals are reported in the upper panel, on an expanded scale.

at the limit of experimental accuracy, was detected for S_{550} values relative to DNA-bound EB); this is consistent with the attribution of high-frequency modes to in-plane vibrations of the macrocycle.

RESULTS AND DISCUSSION

Dynamics of the free chromophore

The temperature dependence of parameters σ^2 and ν_0 relative to EB free in solution is shown in Figs. 3 and 4. The thermal behavior of these parameters is clearly characterized by two distinct regions. At low temperature, the harmonic behavior given by Eqs. 2 and 3 is obeyed: the fitting of the low-temperature data points, relative to both parameters σ^2 and ν_0, in terms of the harmonic model is represented by the solid lines in Figs. 3 and 4, and the parameter values are reported in Table 2. At higher temperatures, clear deviations from the predictions of the harmonic model are observed for both ν_0 and σ^2; these can be taken as evidence of the onset of nonharmonic molecular motions in our system. The onset temperature depends upon the solvent, being 150 K and 180 K for the samples in 80% ethylene glycol/water and in 90% glycerol/water, respectively. The above values are very close to those reported in the literature for the glass transition temperature of the solvent matrix; this suggests that solvent motions are (directly or indirectly) involved in the anharmonicity effect. The data reported in Table 2 characterize the coupling of the electronic transition with the bath of low-frequency harmonic modes. In particular, we note that the average frequency appears to be larger for glycerol/water than for ethylene glycol/water, thus suggesting that the former matrix constitutes a more rigid environment for the free chromophore than the latter. Moreover, large σ_{in} values are observed in both solvents; this can be attributed to a large conformational heterogeneity, likely brought about by different orientations of the phenyl and ethyl groups with respect to the phenanthridinium ring. Quadratic coupling appears to be very small for the chromophore free in solution ($R \approx 1$), whereas the different values of $\nu_{00} + C$ observed in the two solvents reflect the well-known solvent effect on the peak position of the band (see, e.g., Cantor and Schimmel, 1980).

TABLE 1 Values of the parameters that characterize the coupling of the electronic transition with high-frequency modes

	Solvent	S_{550}	S_{1340}	S_{2000}
EB free	80% ET-GLY	1.1 ± 0.1	0.66 ± 0.08	0.08 ± 0.02
EB free	90% GLYC	1.1 ± 0.1	0.70 ± 0.08	0.10 ± 0.02
EB bound	80% ET-GLY	0.8 ± 0.1	0.64 ± 0.08	0.05 ± 0.02
EB bound	90% GLYC	0.9 ± 0.1	0.60 ± 0.08	0.07 ± 0.02

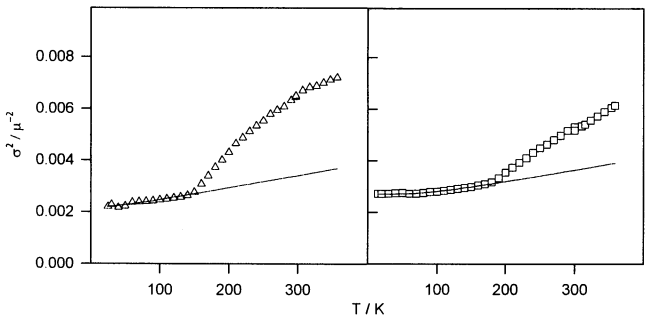

FIGURE 3 Values of parameter σ^2 as a function of temperature for EB free in solution. (*Left*) 80% ethylene glycol/water (△); (*right*) 90% glycerol/water □. The continuous lines represent the fitting of the low-temperature data points in terms of Eq. 2 in the text.

Dynamics of the DNA-bound chromophore

The temperature dependence of parameters σ^2 and ν_0 relative to EB bound to DNA is reported in Figs. 5 and 6 for the two solvent conditions investigated. Again, a low-tempera-

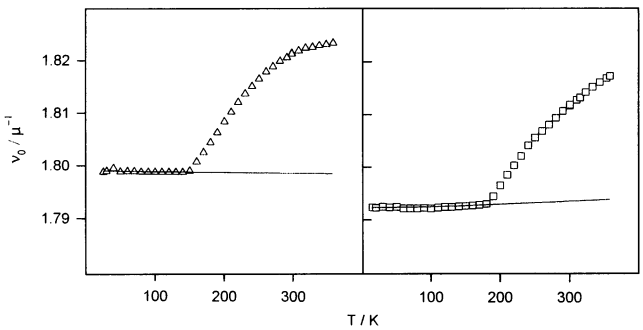

FIGURE 4 Values of parameter ν_0 as a function of temperature for EB free in solution. Panels and symbols are as in Fig. 3. The continuous lines represent the fitting of the low-temperature data points in terms of Eq. 3 in the text.

TABLE 2 Values of the parameters that characterize the coupling of the electronic transition with the "bath" of low-frequency modes

	Solvent	*NS*	$\langle\nu\rangle$/cm^{-1}	σ_{in}/cm^{-1}	*R*	$(\nu_{00} + C)$/cm^{-1}
EB free	80% ET-GLY	4.5 ± 0.5	80 ± 30	440 ± 20	1.0000 ± 0.0001	17991 ± 10
EB free	90% GLYC	2.0 ± 0.5	175 ± 50	460 ± 30	1.0000 ± 0.0001	17916 ± 10
EB bound	80% ET-GLY	2.5 ± 0.5	290 ± 50	<50	0.9980 ± 0.0001	18401 ± 10
EB bound	90% GLYC	3.5 ± 0.5	275 ± 50	<50	0.9980 ± 0.0001	18371 ± 10

ture region, where the harmonic behavior given by Eqs. 2 and 3 is followed, can be clearly identified; the fitting of the low-temperature data points, relative to both parameters σ^2 and ν_0, in terms of the harmonic model is represented by the solid lines, and the parameter values are reported in Table 2. Differences in the dynamics of the free and DNA-bound chromophore are seen already in the low-temperature harmonic region. In fact, the DNA-bound dye is characterized by larger values of the average frequency of the "bath" (parameter $\langle\nu\rangle$) and smaller heterogeneity (parameter σ_{in}). This indicates that the DNA double helix constitutes, at low temperatures, a rather rigid matrix for the intercalated dye, in which low-frequency vibrations are hindered; moreover, the conformational heterogeneity is also greatly reduced, in line with the location of the phenyl and ethyl groups in the minor groove (Tsai et al., 1977; Jain et al., 1977).

At higher temperatures, deviations from the predictions of the harmonic model are again observed, for both parameters ν_0 and σ^2. The anharmonic contributions (also in comparison with those observed for the free chromophore) are better evidenced in Fig. 7, where we report parameter $\Delta\sigma^2$ (i.e., the difference between the measured σ^2 values and the predictions of the harmonic model) as a function of temperature. Up to ~280 K, anharmonic motions are smaller for the DNA-bound than for the free chromophore, and the $\Delta\sigma^2$ versus T slopes are smaller; around 280 K a steep increase is observed for the former, so that at temperatures higher than ~310 K, anharmonic motions become larger for the DNA-bound chromophore. The effect tends to saturate around 350 K, where the DNA double helix has melted.

Functional relevance and solvent dependence

Data in Fig. 7 clearly show that EB dynamics depends upon the physical properties of the matrix in which the chromophore is embedded. In particular for the DNA-bound dye, anharmonic motions, which are initially hindered, become greatly enhanced at temperatures approaching the physiological range. To investigate the functional relevance of these motions and their dependence on the external solvent, $\Delta\sigma^2$ values are reported in Fig. 8, after suitable normalization, in comparison with the DNA melting curves measured under identical experimental conditions. We stress the following points:

1. The steep increase in $\Delta\sigma^2$ values clearly precedes the melting of the DNA double helix; we therefore attribute the anharmonic motions to premelting motions within the double-helical DNA, rather than to the melting of the double helix.

2. The above motions strongly depend upon solvent composition and in 80% ethylene glycol/water occur at lower temperatures than in 90% glycerol/water; the solvent effect on premelting motions is much larger (~20 K) than on the melting itself (~6 K).

3. The anharmonicity effect tends to saturate at temperatures where substantial melting of the double helix is observed; it may be suggested that data points at the highest temperatures in Figs. 7 and 8 reflect the dynamic behavior of the dye bound to single-helical, random-coil DNA. In this respect it must be noted that detachment of the dye from DNA, in our experimental conditions, can be excluded by the data in Figs. 3 and 5. Indeed, it is well known that

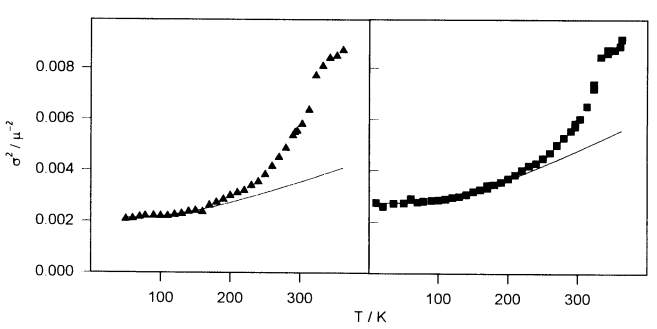

FIGURE 5 Values of parameter σ^2 as a function of temperature for EB bound to DNA. (*Left*) 80% ethylene glycol/water (▲); (*right*) 90% glycerol/water (■). The continuous lines represent the fitting of the low-temperature data points in terms of Eq. 2 in the text.

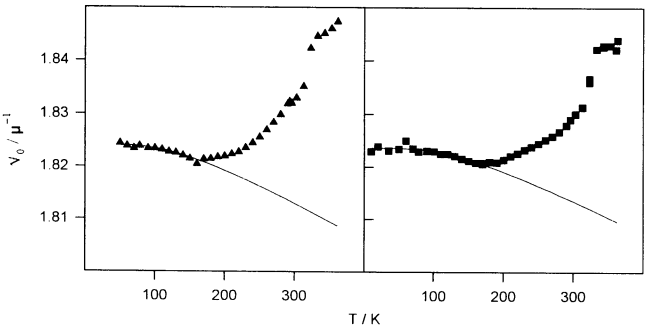

FIGURE 6 Values of parameter ν_0 as a function of temperature for EB bound to DNA. Panels and symbols are as in Fig. 5. The continuous lines represent the fitting of the low-temperature data points in terms of Eq. 3 in the text.

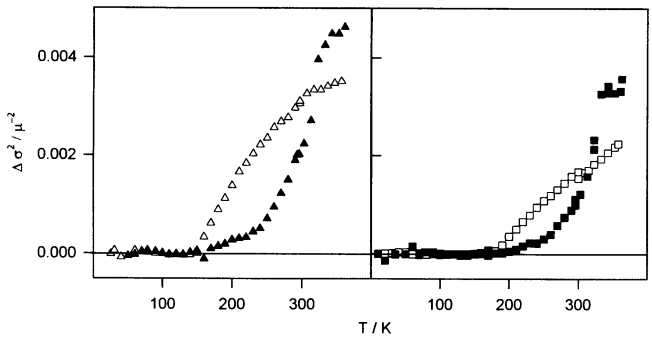

FIGURE 7 Values of $\Delta\sigma^2$ as a function of temperature. $\Delta\sigma^2$ is defined as the difference between the experimental points in Figs. 3 and 5 and the harmonic behavior predicted by Eq. 2 (*continuous lines* in the same figures). △, □, EB free in solution; ▲, ■, EB bound to DNA. (*Left*) 80% ethylene glycol/water (△, ▲); (*right*) 90% glycerol/water (□, ■).

parameter ν_0 (i.e., the peak position of the band) is most sensitive to the environment of the chromophore; however, data in Fig. 5 show that ν_0 values for the DNA-bound dye remain, at high temperatures, around 18,400–18,500 cm^{-1}, very different from the values of ~18,200 cm^{-1} observed for the free chromophore in the same solvents at the same temperatures.

CONCLUSIONS

The data reported in this work confirm that the temperature dependence of the optical lineshape is a sensitive probe of the local dynamics in the proximity of the chromophore. Moreover, comparison of the thermal behavior of the chromophore free in solution and bound to a macromolecule makes it possible to obtain information on the local dynamic properties of the macromolecule itself. The question now arises about the kind of motions that are responsible for the observed effects. To this purpose, we recall that because we are using optical absorption spectroscopy, we are able to detect only nuclear motions coupled to the electronic transition responsible for the absorption band investigated. In the present case, because the observed EB absorption band arises from a $\pi \rightarrow \pi^*$ electronic transition within the phenanthridinium ring, our experimental technique can detect only nuclear motions that take place with respect to the planar ring structure of the chromophore (and for this reason the term "local dynamics" is used throughout this work), whereas motions in which the probe and the nearby atoms from the macromolecule move in phase (e.g., translations, rotations, or torsional dynamics of the double helix) remain undetected; this is at odds with other experimental techniques (e.g., fluorescence decay or fluorescence anisotropy decay in the nanosecond time scale) that are particularly sensitive to this last type of motion (Collini et al., 1995). For a deeper discussion on the dynamic information that can be obtained with optical spectroscopy, in comparison with that obtained with other experimental techniques, see Melchers et al. (1996).

In view of the above arguments, we attribute the anharmonic motions responsible for the reported $\Delta\sigma^2$ effect (see Figs. 6 and 7) to premelting motions within the double-helical DNA, e.g., local opening or unwinding of the double helix; the onset of such motions within the double helix may also allow an increased wobbling of the chromophore inside its intercalation site. We also suggest that these motions can be relevant to the functional properties of DNA (replication and transcription); it is very interesting to stress the rather large solvent effect observed on $\Delta\sigma^2$ (Fig. 7), which suggests a role of the microenvironment in local anharmonic motions and functional properties of the DNA double helix. It may also be suggested that the above solvent-dependent motions can be invoked to explain the discrepancy between the measured amount of fluorescence anisotropy decay at 100 ps (Magde et al., 1983; Härd et al., 1989) and the value calculated with "in vacuo" harmonic dynamics (Rudolph and Case, 1989). A final warning must also be given, concerning the effect of the intercalated probe on the reported DNA dynamics; in fact, the rather high [EB]/[DNA] concentration ratio (approximately one intercalated EB molecule for every 10 base pairs) used in this study could cause an enhancement of the double-helix rigidity. However, it should be stressed that normal-mode analysis shows that intercalation of ethidium has only minor effects on the vibrational motions of the surrounding base pairs and that the motions of ethidium provide a good probe of the surrounding motions (Rudolph and Case, 1989).

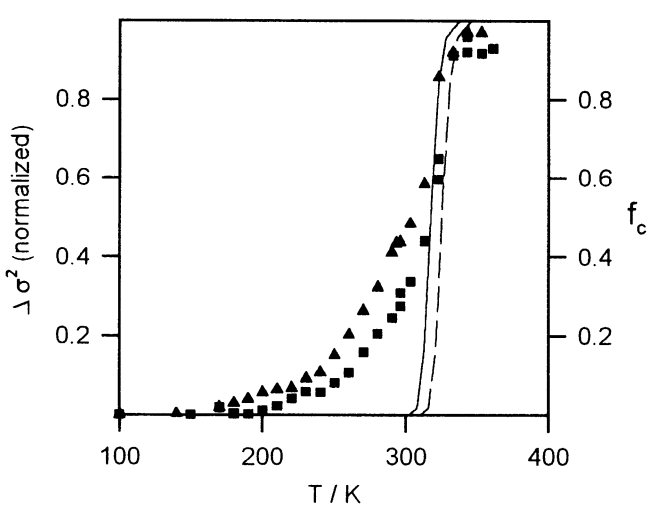

FIGURE 8 Comparison of normalized $\Delta\sigma^2$ values relative to DNA-bound EB (*left scale*) with the DNA melting curves (fraction of denatured DNA, f_C; *right scale*). Symbols are as in Fig. 7. ——, Melting curve in 80% ethylene glycol/water; – – –, melting curve in 90% glycerol/water. The melting curves were measured under experimental conditions identical to those under which the $\Delta\sigma^2$ values were measured.

The authors thank Dr. M. Leone for useful discussions and comments and for critical reading of the manuscript, and Mr. G. Lapis and Mr. F. D'Anca for technical help with the cryogenic measurements.

General indirect support to this work has also been provided by the Comitato Regionale Fisica Nucleare e Struttura della Materia (CRRNSM).

REFERENCES

Baldini, G., and G. Varani. 1985. The role of the solvent on the binding of ethidium bromide to DNA in alcohol-water mixtures. *Biopolymers.* 25:2187–2208.

Baldini, G., and G. Vegetti. 1989. Low temperature spectroscopy of DNA-intercalator ethidium. *J. Lumin.* 43:41–49.

Boffi, A., E. Chiancone, D. Verzili, L. Cordone, A. Cupane, M. Leone, V. Militello, E. Vitrano, E. E. Di Iorio, and W. Yu. 1994. Stereodynamic properties of the cooperative homodimeric *Scapharca inaequivalvis* hemoglobin studied through optical absorption spectroscopy and ligand rebinding kinetics. *Biophys. J.* 67:1713–1723.

Bresloff, J. R., and D. M. Crothers. 1975. DNA/ethidium reaction kinetics: demonstration of direct ligand transfer between DNA binding sites. *J. Mol. Biol.* 95:103–123.

Cantor, C. R., and P. R. Schimmel. 1980. Biophysical Chemistry, Part II. W. H. Freeman and Co., San Francisco. 386–389.

Chinsky, L., P. Y. Turpin, and M. Duquesne. 1976. Resonance Raman spectra of highly fluorescent molecules: free and DNA-bonded ethidium bromide. Proceedings of the 5th International Conference on Raman Spectroscopy. E. D. Scneider, J. Brand Muller, W. Kiefer, B. Schrader and H. W. Schrotter, editors. Schulz, Freiburg. 196–197.

Collini, M., G. Chirico, G. Baldini, and M. E. Bianchi. 1995. Conformation of short DNA fragments by modulated fluorescence polarization anisotropy. *Biopolymers.* 36:211–225.

Cordone, L., A. Cupane, M. Leone, and E. Vitrano. 1986. Optical absorption spectra of deoxy- and oxy-hemoglobin in the temperature range 300–20 K. Relation with protein dynamics. *Biophys. Chem.* 24: 259–275.

Cupane, A., M. Leone, L. Cordone, H. Gilch, W. Dreybrodt, E. Unger, and R. Schweitzer-Stenner. 1996. Conformational properties of nickel(II) octaethylporphyrin in solution. 2. A low-temperature optical absorption spectroscopy study. *J. Phys. Chem.* 100:14192–14197.

Cupane, A., M. Leone, V. Militello, M. E. Stroppolo, F. Polticelli, and A. Desideri. 1994. Low temperature optical spectroscopy of native and azide reacted Cu, Zn bovine superoxide dismutase. A structural dynamics study. *Biochemistry.* 33:15103–15109.

Cupane, A., M. Leone, V. Militello, M. E. Stroppolo, F. Polticelli, and A. Desideri. 1995a. Low temperature optical spectroscopy of cobalt in Cu, Co superoxide dismutase. A structural dynamics study of the solvent unaccessible metal site. *Biochemistry.* 34:16313–16319.

Cupane, A., M. Leone, E. Vitrano, and L. Cordone. 1995b. Low temperature optical absorption spectroscopy: an approach to the study of stereodynamic properties of hemeproteins. *Eur. Biophys. J.* 23:385–398.

Cupane, A., M. Leone, E. Vitrano, L. Cordone, U. R. Hiltpold, K. H. Winterhalter, W. Yu, and E. E. Di Iorio. 1993. Structure-dynamics-function relationships in Asian elephant (*Elephas maximus*) myoglobin. An optical spectroscopy and flash-photolysis study on functionally important motions. *Biophys. J.* 65:2461–2472.

Di Pace, A., A. Cupane, M. Leone, E. Vitrano, and L. Cordone. 1992. Protein dynamics: vibrational coupling, spectral broadening mechanisms and anharmonicity effects in carbonmonoxy heme proteins studied by the temperature dependence of the Soret band lineshape. *Biophys. J.* 63:475–484.

Giacomoni, P. U., and M. Le Bret. 1973. Electronic structure of ethidium bromide. *FEBS Lett.* 29:227–230.

Härd, T., P. Fan, D. Magde, and D. R. Kearns. 1989. On the flexibility of DNA: time-resolved fluorescence polarization of intercalated quinacrine and 9-amino-6-cloro-2-methoxyacridine. *J. Phys. Chem.* 93:4338–4345.

Jain, S. C., C. C. Tsai, and H. M. Sobell. 1977. Visualization of drug-nucleic acid interactions at atomic resolution. II. Structure of an ethidium/dinucleoside monophosphate crystalline complex, ethidium: 5-iodocytidylyl (3′-5′) guanosine. *J. Mol. Biol.* 114:317–331.

Leone, M., A. Cupane, and L. Cordone. 1996. Low temperature optical spectroscopy of low spin ferric heme proteins. *Eur. Biophys. J.* 24: 117–124.

Leone, M., A. Cupane, V. Militello, and L. Cordone. 1994. Thermal broadening of Soret band in heme complexes and in heme-proteins: role of the iron dynamics. *Eur. Biophys. J.* 23:349–352.

Lybrand, T., and P. Kollman. 1985. Molecular mechanical calculations on the interaction of ethidium cation with double-helical DNA. *Biopolymers.* 24:1863–1879.

Magde, D., M. Zappala, W. H. Knox, and T. M. Nordlund. 1983. Picosecond fluorescence anisotropy decay in the ethidium/DNA complex. *J. Phys. Chem.* 87:3286–3288.

Melchers, B., E. W. Knapp, F. Parak, L. Cordone, A. Cupane, and M. Leone. 1996. Structural fluctuations of myoglobin from normal modes, Mössbauer-, Raman- and absorption-spectroscopy. *Biophys. J.* 70: 2092–2099.

Militello, V., A. Cupane, M. Leone, W. S. Brinigar, A. L. Lu, and C. Fronticelli. 1995. Dynamic properties of some β-chain mutant hemoglobins. *Proteins.* 22:12–19.

Nuutero, S., B. S. Fujimoto, P. F. Flynn, B. R. Reid, N. S. Ribeiro, and J. M. Schurr. 1994. The amplitude of local angular motion of purines in DNA in solution. *Biopolymers.* 34:463–480.

Rudolph, B. R., and D. A. Case. 1989. Harmonic dynamics of a DNA hexamer in the absence and presence of the intercalator ethidium. *Biopolymers.* 28:851–871.

Schomacker, K. T., and P. M. Champion. 1986. Investigations of spectral broadening mechanisms in biomolecules: cytochrome *c*. *J. Chem. Phys.* 84:5314–5325.

Schomacker, K. T., and P. M. Champion. 1989. Investigations of the temperature dependence of resonance Raman cross sections: applications to heme proteins. *J. Chem. Phys.* 90:5982–5993.

Shibata, J. H., B. S. Fujimoto, and J. M. Schurr. 1985. Rotational dynamics of DNA from 10^{-10} to 10^{-5} seconds: comparison of theory with optical experiments. *Biopolymers.* 24:1909–1930.

Tsai, C. C., S. C. Jain, and H. M. Sobell. 1977. Visualization of drug-nucleic acid interactions at atomic resolution. I. Structure of an ethidium/dinucleoside monophosphate crystalline complex, ethidium: 5-iodouridylyl (3′-5′) adenosine. *J. Mol. Biol.* 114:301–315.

Varani, G., L. Della Torre, and G. Baldini. 1987. Nonspecific interactions in dye binding to DNA. Influence of alcohols and amides. *Biophys. Chem.* 28:175–181.